PR7

Development on Neutron Imaging Application

Y. Saito

Institute for Integrated Radiation and Nuclear Science, Kyoto University

OBJECTIVES and ALLOTED RESEARCH SUBJECT: Neutron imaging provides valuable information which cannot be obtained from an optical or X-ray imaging. The purpose of this project is to develop the imaging method itself and the experimental environment for expanding the application area of the neutron imaging. The allotted research subjects are as follows:

ARS-1: Measurements of Multiphase Dynamics by Neutron Radiography (Y. Saito et al.)
ARS-2: Visualization of Liquid Water Behavior in a Polymer Electrolyte Fuel Cell under High Temperature Operation (H. Asano et al.)
ARS-3: Trial Visualization of Quenching Phenomena in Vertical Hole (H. Umekawa et al.)
ARS-4: Evaluation of Meltwater Penetration During Defrosting Process (R. Matsumoto et al.)
ARS-5: Effect of the water content of concrete on the spalling phenomenon (M. Kanematsu et al.)
ARS-6: Neutron Radiography on the Effects of a Mixer with an Inserted Tube in a Flow-type Supercritical Hydrothermal Reactor (S. Takami et al.)
ARS-7: Visualization of plant roots in media containing organic matter using neutron CT (U. Matsushima et al.)
ARS-8: Development of a method for quantitative estimation of neutron imaging (M. Kitaguchi et al.)
ARS-9: In-situ Observation of Electrolyzed Lithi-um-ion Conductor through Neutron Radiography (S. Takai et al.)
ARS-10: Flow Visualization of Coolant inside Layered Rod Array (Kaneda et al.)

MAIN RESULTS AND THE CONTENTS OF THIS REPORT:

ARS-1 performed visualization of boiling two-phase flow by high-speed imaging. The dynamics of the two-phase flow pattern in a tube were analyzed based on its spatio-temporal distribution.

ARS-2 applied to neutron imaging to water accumulation in Polymer Electrolyte Fuel Cell (PEFC). In this study, the water content and its distribution were visualized at a cell temperature of 105 °C.

ARS-3 investigated the quenching phenomena. Results expresses the influence of the restriction caused by the counter current flow limitation (CCFL) condition clearly.

ARS-4 evaluates the meltwater penetration during defrosting process, which is one of the important phenomena to enhance the energy efficiency of the air conditioning system.

ARS-5 applied the spalling phenomenon of concrete from the perspective of its internal moisture.

ARS-6 proposed a mixer for the instantaneous heating of the reactant solution and performed neutron radiography measurements to confirm how the fluids mixed in the proposed mixer.

ARS-7 applied neutron CT to visualization of plant roots in media containing organic matter. It was demonstrated that root distribution can be observed by supplying D_2O to the roots.

ARS-8 applies the electric field to the model cell to observe the lithium migration in the solid electrolyte employing the NR.

ARS-9 was not performed due to the difficulties to set up experiments in 2023.

ARS-10 performed the visualization of coolant inside the layered rod array. From the experimental results, it was found the profile of the coolant inside the structure depends on the pouring liquid temperature and flowrate rather than the applied heat on the structure.

PR7-1

Measurements of multiphase flow dynamics using neutron radiography

Y. Saito, D. Ito and N. Odaira

Institute for Integrated Radiation and Nuclear Science, Kyoto University

INTRODUCTION: Neutron radiography (NRG) is useful for visualizing multiphase flow. It can also measure the flow structure and dynamics of boiling two-phase flow. This study aims to investigate changes in the flow pattern of boiling two-phase flow in a heated pipe using NRG and to clarify its dynamics by analyzing temporal fluctuations. NRG proves effective in understanding thermal-hydraulic phenomena in metallic pipes due to its high transmissivity and has been applied in various applications. While most previous studies have focused on average characteristics [1], measuring spatio-temporal characteristics can provide new insights using a high-speed imaging system.

EXPERIMENTS: Experiments were conducted in the B-4 facility of KUR. A high-speed imaging system comprising an optical image intensifier and a high-speed camera was employed to acquire sequences of neutron transmission images of boiling flow at 1000 fps. The test section featured a stainless-steel tube with an inner diameter of 10 mm, heated by Joule heating. The cross-sectional average void fraction was calculated from the instantaneous void fraction distribution estimated from the transmission images. The dynamics of the flow pattern in the tube were analyzed based on its spatio-temporal distribution.

RESULTS: A typical result of the spatio-temporal distribution of measured void fraction is shown in Fig. 1. In the middle of the heated section, bubble generation begins, and the rise of bubbles is observable in the distribution. In the upper part of the tube, the flow changes to the annular flow, and the movement of the liquid film appears as stripes. Thus, understanding the dynamic characteristics of the flow structure and identifying the pattern can be achieved by estimating characteristic quantities from it.

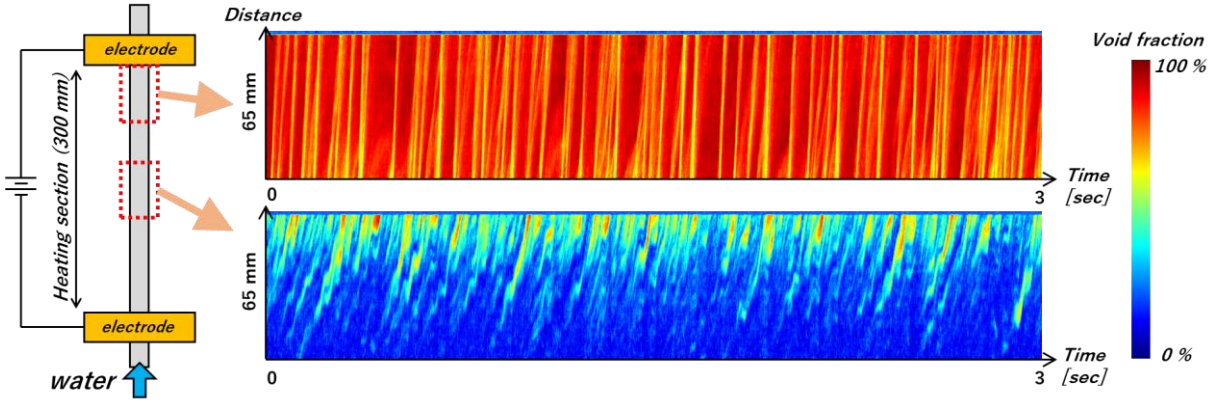

Fig. 1 Spatio-temporal distributions of cross-sectional averaged void fraction in a heated tube (q = 290 kW/m^2, G = 200 kg/s, ΔT_{sub} = 20 K)

REFERENCES:

[1] T. Ami *et al.*, Exp. Therm Fluid Sci., **141** (2023) 110799.

Visualization of Liquid Water Behavior in a Polymer Electrolyte Fuel Cell under High-Temperature Operation

H. Murakawa, Y. Obayashi, K. Nakagawa, K. Sugimoto, H. Asano, Y. Shirase[1], C. Schreiber[1], S. Wakolo[1], E. Dzramado[1], J. Inukai[1], D. Ito[2] and Y. Saito[2]

Department of Mechanical Engineering, Graduate School of Engineering, Kobe University
[1]Hydrogen and Fuel Cell Nanomaterials Center, University of Yamanashi
[2]Institute for Integrated Radiation and Nuclear Science, Kyoto University

INTRODUCTION: Polymer electrolyte fuel cells (PEFCs) are expected to be used in the electrification of heavy-duty vehicles (HDVs), but higher operating temperatures are required to accommodate higher power outputs and smaller cooling systems. Currently, the practical realization of fuel cells with an operating temperature of about 120 °C is being considered [1], but in this case, to prevent dryout, the saturation temperature of the water must be increased, i.e., the pressure in the fuel cell must be increased. The formation of liquid water in a fuel cell is determined by humidity, temperature and the amount of water produced by the cell reactions, which may depend on their spatial distribution when accompanied by cell reactions. In this study, the water content and its distribution were visualized at a cell temperature of 105 °C under various pressure condition by neutron radiography.

EXPERIMENTS: A small single-cell PEFC with a reaction area of 20×20 mm^2 was used. Humidified hydrogen gas and air were supplied to the anode and cathode through ten parallel straight channels with the cross-section of 1×1 mm^2, respectively. The width of ribs was 1 mm. The thickness of the PEM including the catalyst layer was 200 μm and the thickness of the GDL was 235 μm. The pressure in the anode and cathode of the PEFC was maintained by regulating valves in the exhaust line. The PEFC was placed in the vertical plane and the gas flows in the anode and cathode formed counter-current flow. The air flow in the cathode was a vertical downward flow. Hydrogen gas and air were supplied to the anode and cathode at a humidification temperature of 74.6 °C and a flow rate of 200 cc, respectively. The imaging was carried out with an exposure time of 30 s during the reactor operation at 1 MW output.

RESULTS: The cell voltage was measured when the current density was varied from 0, 0.4, 0.6, 0.8 and 1.0 mA/m^2 under the condition of the pressure in the PEFC of 250 kPa. The relative humidity of the supplied gas was 34.2 % at the inlet of the PEFC. Steady-state conditions were obtained up to a current density of 0.8 mA/m^2, but at 1.0 mA/m^2, a decrease and fluctuation of the cell voltage was observed. The measured results of water thickness are shown in Fig. 1(a) to (c). At 80 minutes after the measurement start, just before the current density was increased to 1.0 mA/m^2, little increase in the water film thickness was observed. At 88 minutes, Liquid water began to drain into the channel from the corner at the base of the ribs, and then, the liquid water in the channels gradually increased. At 100 minutes, it was confirmed that some liquid water plugs were formed in the channels. Such liquid water plugs interfered with the supply of the reaction gas and led to a drop in the cell voltage.

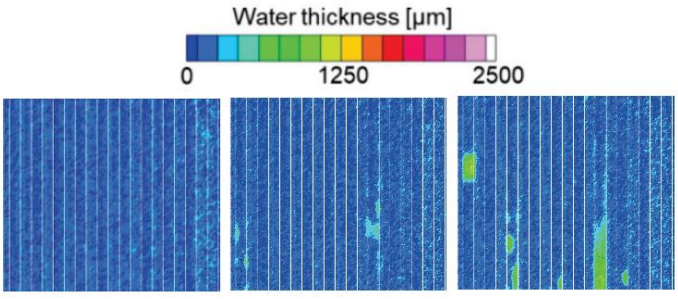

(a) 80 minutes (b) 88 minutes (c) 100 minutes

Fig. 1. Water thickness distribution.

REFERENCES:

[1] J. Zhang *et al.,* Electrochimica Acta, **52**(15) (2007) 5095-5101.

Trial Visualization of Quenching Phenomena in Vertical Hole

H. Umekawa, T. Ami, R. Tujimoto, Y.Saito[1], D.Ito[1] and N.Odaira[1]

Department of Mechanical Engineering Kansai University
[4]Institute for Integrated Radiation and Nuclear Science, Kyoto University

INTRODUCTION: The continuous feeding of cool water to the hot surface is one of the key points of the quenching phenomena. These phenomena are widely observed in several industrial instrument, and also in the sever accident of nuclear reactor. Especially in the case of the sever accident, the water must be feed through the complex structure to the hot surface as like as the case of TMI. In this trial, the visualization of the cooling of the hot closed bottom end tube was conducted. Results expresses the influence of the restriction caused by CCFL condition at the channel inlet clearly.

EXPERIMENTS: Figure 1 is the schematic diagram of the experimental apparatus. Firstly, the test section is heated up a.800 deg.C by installing into the electric farness. When the temperature reached the predetermined value, testsection is pull up, and the Head tank water enter to the receiver by opening of Electric valve. During the quenching, flow structure is recorded by using the highspeed camera (250fps exposure period 1/900). Sheathed thermocouples is fixed upon the test section surface by using wire, and the data is recorded by data logger (10Hz). The example of cooling curve is shown in Fig.2, and succeed visualization images are shown in Figs. 3(a) and (b). Owing to the restriction at the tube inlet in small diameter tube, liquid is kept at the top region. As the results, quenching period of small diameter tube takes the longer period compared with the large tube. Even in the case of the large diameter tubes, the restriction caused by the CCFL condition at the inlet of the tube, but This restriction is intermitted and the inverted annular flow is observed in the visualization results.

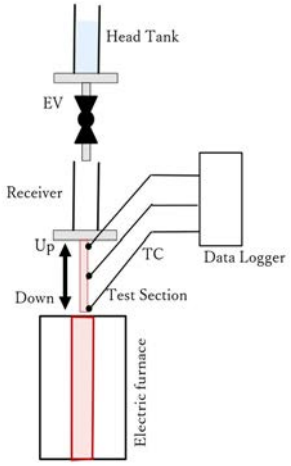

Fig.1 Experimental apparatus

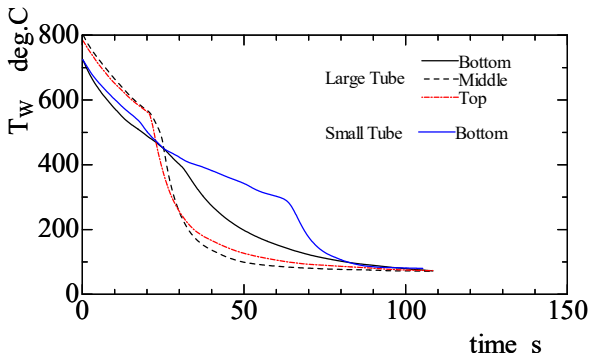

Fig 2 Example of Cooling curves

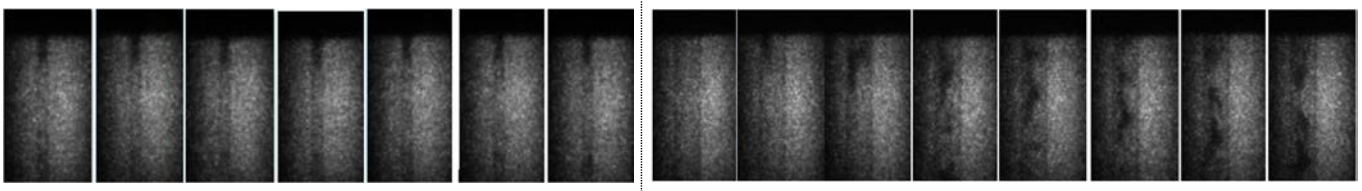

(a) Small Tube (b) Large Tube

Fig.3 Example of flow Visualization (250fps)

PR7-4

Evalulation of Meltwater Penetration During Defrosting Process

S. Kimura, R. Matsumoto [1], K. Kida, Y. Shirotani[1], K. Kobayasi[1], Y. Saito[2] D. Ito[2] and N. Odaira[2]

Graduate School of Science and Engineering, Kansai University
[1]Faculty of Engineering Science, Kansai University
[2]Institute for Integrated Radiation and Nuclear Science, Kyoto University

INTRODUCTION: Frost formation on the heat exchangers of the air conditioning system causes the serious problem on the heat transfer performance. In order to recover the performance of the heat exchanger, a defrosting operation is performed periodically to remove the frost from the heat exchanger by flowing hot gas through the heat transfer tubes. Matsumoto et al. [1] reported the removal of meltwater by penetrating into the remaining frost layer. By using this phenomenon, effective defrosting can be achieved. However, the relationship between the penetration speed of the meltwater and the temperature distribution on the frosting plate is not clear. In this study, the behavior of meltwater was estimated by neutron radiography.

EXPERIMENTS AND RESULTS: Frost was formed on the aluminum plate with a thickness of 0.5 mm by cooling it down to -25 °C. A temperature gradient was applied by raising the temperature at one edge of the plate to 5°C, thus, the defrosting was performed in one direction. The defrosting duration was 15 min. The water penetration image at 7 min after the start of defrosting is shown in Fig.1, where defrosting was occurred from left to right, and melted water can be seen in the center of the plate with a water penetration width of approximately 5 mm. The water distribution of the rectangular area indicated by the orange line was extracted and rearranged for each defrosting time in Fig. 2. The vertical axis in Fig. 2 is the direction of meltwater penetration and the horizontal axis is the time elapsed since defrosting. Figure 2 shows that defrosting occurs at a constant speed while increasing the penetration width, and that the frost layer in the penetration zone can hold up to about twice its own water content. The visually observed penetration front, indicated by the circle plot, is in agreement with the results of the neutron radiography observation. The temperature distribution was measured by 11 thermocouples attached to the back of the aluminum plate. The temperature of the penetration front shows 0°C.

REFERENCES:

[1] R. Matsumoto *et al.,* Transactions of the Japan Society of Refrigerating and Air Conditioning Engineers, **37(3)** (2020) 249.

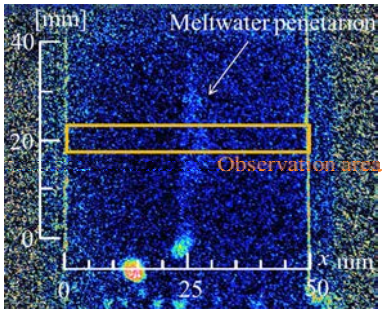

Fig. 1 Water penetration image.

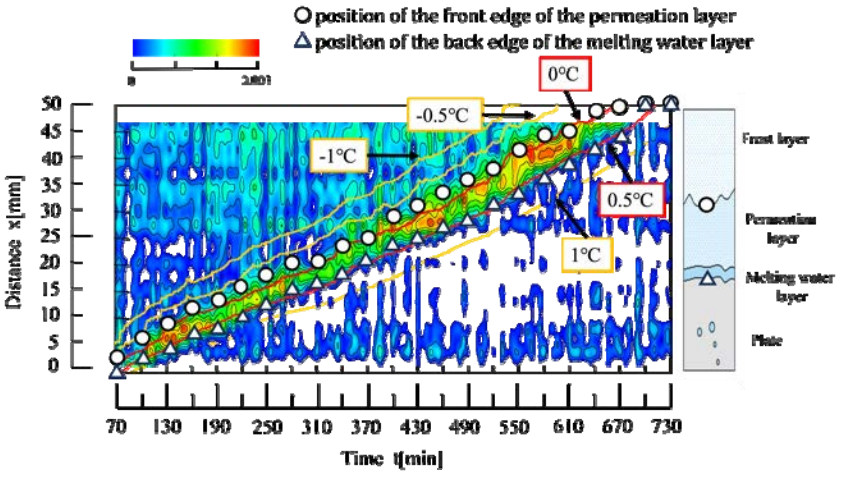

Fig. 2 Spatio-temporal distribution of meltwater penetration .

PR7-5

Effect of the water content of concrete on the spalling phenomenon

M. Kanematsu[1], Y. Nishio[2], J. Kim[1], N. Odira[3], D. Ito[3], Y. Saito[3]

[1]*Department of Architecture, Tokyo University of Science*
[2]*Building Research Institute*
[3]*Institute for Integrated Radiation and Nuclear Science, Kyoto University*

INTRODUCTION: This study aimed to understand the spalling phenomenon of concrete from the perspective of its internal moisture. Capturing detailed moisture movement in concrete under fire is essential to understanding the spalling mechanism [1]. Therefore, the explosion tendency according to the change in the internal moisture state is identified, and the effect of the change in the pressure state due to the condensation of moisture on the explosion is examined by using neutron radiography.

EXPERIMENTS: The size of the test specimen is 100 × 70 × 30 mm, shown in Fig.1. Additionally, to measure the internal pressure, the pipes for pressure measurement and thermocouples were molded at 10mm and 20mm from the heating surface. Neutron radiography was performed at TNRF in the B-4 port of KUR.

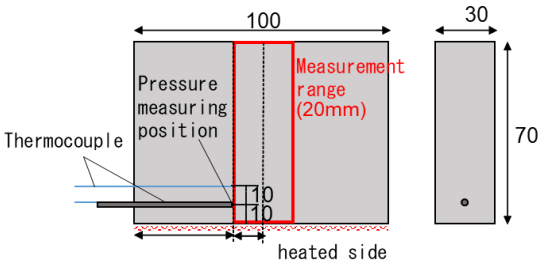

Figure 1. Pressure and temperature measurement location of the specimen

RESULTS: Our findings, as depicted in Figure 2, reveal the relative moisture content distribution after 5 minutes of heating for concrete with varying initial moisture contents. Notably, at the 53% and 87% initial relative moisture content levels, we observed the moisture clog phenomenon, where the moisture content exceeded the initial moisture content, in areas distant from the heated surface. Considering that spalling was observed in specimens with an initial moisture content of 40-95% in excess of 90%, we can infer that the moisture clog is linked to the spalling tendency of these specimens.

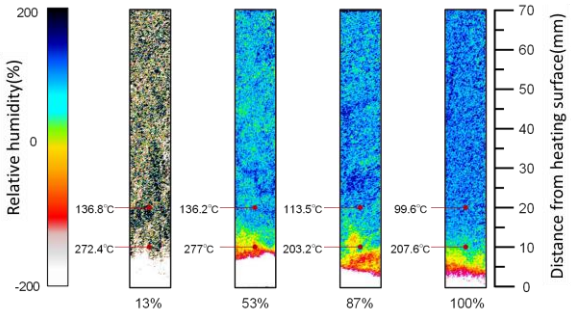

Figure 2. Moisture content after 5 minutes of heating in concrete with different initial moisture contents.

Figure 3 shows the maximum pressure values after 10 minutes of heating. The pressure at 10 mm from the heating surface was mostly less than 1 MPa. This trend is similar to the previous report [2], confirming that the maximum pressure inside the specimen where spalling did not occur was less than 1 MPa

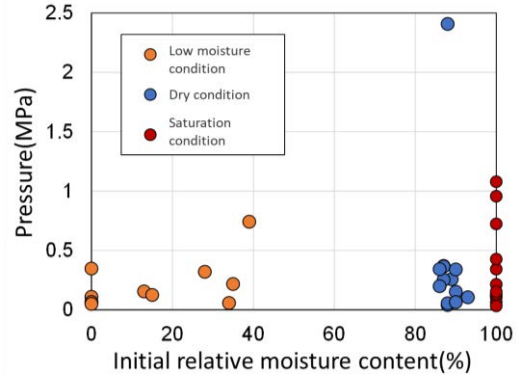

Figure 3. Relationship between maximum pressure and relative moisture content at 10mm from the heating surface

REFERENCES:

[1] JCI-TC-154A (2017). "Committee Reports:"
[2] T. Tanibe, (2014). "Ring restraining testing and spalling index of concrete at high temperature"

Neutron Radiography on the Effects of a Mixer with an Inserted Tube in a Flow-type Supercritical Hydrothermal Reactor

R. Sasaki, T. Kurono, S. Takami, M. Kubo[1], K. Sugimoto[2], N. Odaira[3], D. Ito[3] and Y. Saito[3]

Graduate School of Engineering, Nagoya University
[1]Graduate School of Engineering, Tohoku University
[2]Graduate School of Engineering, Kobe University
[3]Institute for Integrated Radiation and Nuclear Science, Kyoto University

INTRODUCTION: Supercritical hydrothermal synthesis is a method to produce metal oxide nanoparticles in supercritical water. During supercritical hydrothermal synthesis using flow-type reactors, a stream of metal ion aqueous solution was instantaneously heated by mixing with a stream of heated water in a mixer. The previous studies indicated that a mixer with an inserted tube promoted faster mixing of reactant solutions with a stream of heated water. In this study, we tired various sizes of inserted tubes to observe how supercritical water and room-temperature water mixed in the mixer.

EXPERIMENTS: In this study, we conducted neutron radiography measurements to visualize the mixing behavior in a flow-type reactor under operation. The measurements were performed at the B4 port of the Kyoto University Reactor (KUR). The KUR was operated at a 1 or 5 MW output with a neutron flux of ca. 1 or 5×10^7 n/cm^2 s at the beam exit of the B4 neutron guide tube. The experimental setup was similar to that used in previous studies.[1-4] The neutron radiography images were processed to obtain images of the average water density in the mixer.

RESULTS: Figs. 1a, 1c, and 1e show the shape of the mixers with an inserted tube. In this study, we used 1/4-inch T-junction component (Fig. 1a) and a tube with the diameter of 1/8 or 1/16 inch was inserted (Figs. 1c and 1e) from side to supply room temperature water. The observed averaged water density water was shown in Fig. 1b, 1d, and 1f. In the original 1/4-inch T-junction, the room temperature water flowed from side went downward on the right side of the tube (Fig. 1b). When a 1/8-tube was inserted (Fig. 1c), the room temperature water was released from the end of the tube and mixed with the heated water from the top. On the other hand, the insertion of a 1/16-inch tube resulted in the collision of the room temperature water with the left side of wall in the mixer. These results showed that the mixing of the heated water and room temperature water is controlled by the size of side tube and the insertion of 1/8-inch tube realized the most uniform mixing.

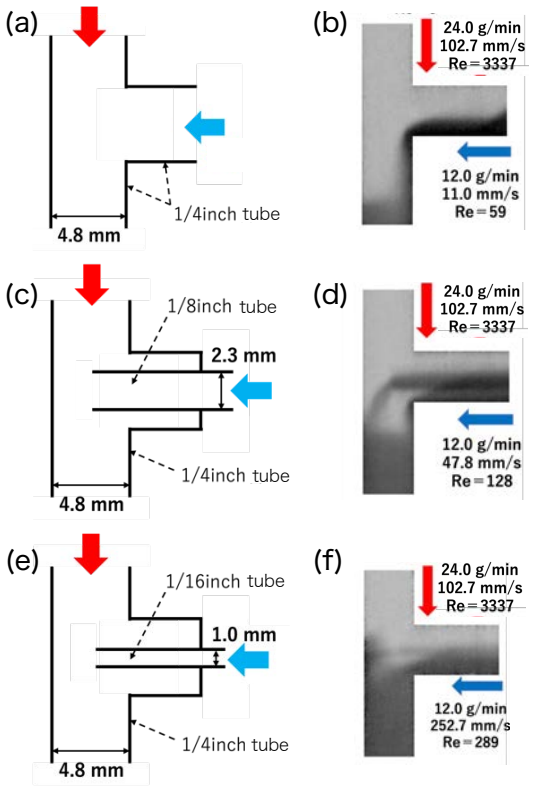

Fig. 1. (a, c, e) Shape of the mixers and (b, d, f) averaged water density in the mixer.

REFERENCES:

[1] K. Sato *et al.*, Chem. React. Eng., **8** (2023) 1449-1456.
[2] R. Sasaki *et al.*, J. Phys.: Conf. Ser., **2605** (2023) 012029.
[3] K. Sugioka *et al.*, AIChE J., **60** (2014) 1168-1175.
[4] S. Takami *et al.*, Phys. Proc., **69** (2015) 564-569.

Visualization of plant roots in media containing organic matter using neutron CT

U. Matsushima[1], N. Odaira[2], D. Ito[2], Y. Saito[3]

Iwate University
Graduate School of Science, Kyoto University

INTRODUCTION: Heavy water (D_2O), which can be readily absorbed by plant roots and creates a contrast between the water in the soil, can be used to visualize roots. This study aimed to utilize heavy water (D_2O) as a contrast agent to visualize plant roots in soil with high organic matter con-tent using neutron computed tomography (CT).

EXPERIMENTS: A rice husk medium containing organic matter (rice husk: soil = 3:1 by volume) was used as the medium, which filled inside aluminum growing containers and planted with a plant sample of komatsuna (*Brassica rapa*). Neutron CT images were acquired using a neutron CT imag-ing system installed in the B4 experimental hole in the KUR research reactor at the Institute for Integrated Radiation and Nuclear Science, Kyoto University. Neutron CT was performed before and after introducing deuterium oxide (D_2O) into the experimental setup. D_2O was supplied only to the roots extending beyond the boundaries of the growing container.

RESULTS: In the image of neutron CT volume data sliced vertically on the surface of the medium (surface image), a shape resembling that of the plant roots observed in the surface image of the medium was observed (Fig. 1-A-a). In contrast, the central image, which is a vertical slice of the volume data at the center of the container, displays a circular image of red-brick soil grains and a filament-like image of the plant roots or surrounding rice husks (Fig. 1-B-a). However, it was chal-lenging to determine whether the filament-like images originated from rice husks or plant roots. Upon introducing D_2O to the roots, a decrease in the pixel values was observed in the region from the bottom to approximately one-third of the vertical direction in both the surface and central images (Fig. 1-A-b, Fig. 1-B-b). In particular, the root image (arrow 1) became invisible after the heavy water supply. In this region, the water content of the roots was replaced by D_2O due to the absorption of water by the plant, which may have increased neutron permeability. A re-gion exhibiting increased neutron transmission was also observed from the bottom of the container to the maximum height of 50 mm (Fig. 1-A-d a, 1-B-d). It was demonstrated that root distribution can be observed in a medium containing organic materials by supplying D_2O to the roots, thereby preventing its diffusion in the medium.

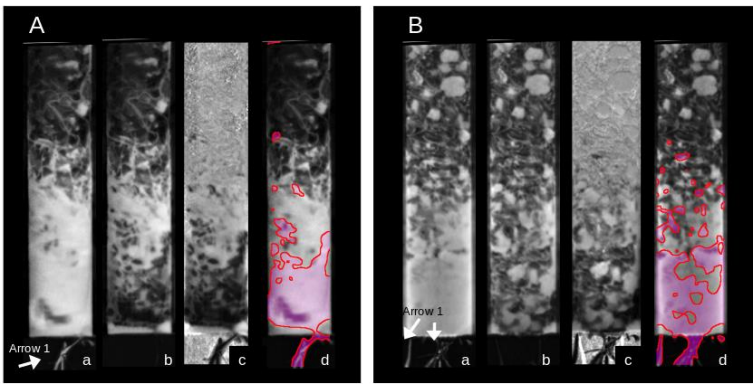

Fig. 1: Slice image of CT volume data of rice husk culture planted with komatsuna. A: surface image, B: central im-age, a, b: pre- and post-D_2O supply, c: The difference be-tween the pre- and post-D_2O supply, d: The difference im-age was binarized and superimposed on the image before introducing D_2O

In-situ Observation of Electrolyzed Lithium-ion Conductor through Neutron Radiography

S. Takai[1], H. Takagi[1], T. Yabutsuka[1], T. Yao[2], D. Ito[3], and Y. Saito[3]

[1]*Graduate School of Energy Science, Kyoto University*
[2]*Kyoto University*
[3]*Institute for Integrated Radiation and Nuclear Science, Kyoto University*

INTRODUCTION: Lithium-ion conductors are presently attracting much interest for the application of solid electrolytes for All-solid-state batteries. While the Li+ ions migrate from the anode to the cathode through the electrolyte during working, the diffusion of lithium-ion is hardly detectable due to the light element. We have carried out the lithium diffusion coefficient measurement using the neutron radiography (NR) technique. Utilizing the large difference in the neutron attenuation factors between ^{6}Li and ^{7}Li, we have measured the diffusion coefficient from the isotope diffusion profiles of the annealed samples.

In the present study, we applied the electric field to the model cell to observe the lithium migration in the solid electrolyte employing the NR.

EXPERIMENTS: ^{7}Li-LAGP ($Li_{1.5}Al_{0.5}Ge_{1.5}(PO_4)_3$ using ^{7}Li) solid electrolyte and ^{6}Li-LMO ($LiMn_2O_4$ using ^{6}Li) electrode material were prepared by the conventional solid-state reaction method. Test cell with Cu/^{6}Li-LMO/PEO/^{7}Li-LAGP/PEO/^{6}Li-LMP/Al was constructed, which were heated up to 140°C and electrolyzed by using a galvanostat with 28.8 – 86.4 μA of current. The mounted amount of cathode and anode materials are 3 and 6 mg, respectively. Before, after, and during the electrolysis, NR data were collected by CCD camera at the B4 guide tube in IIRNS, Kyoto University.

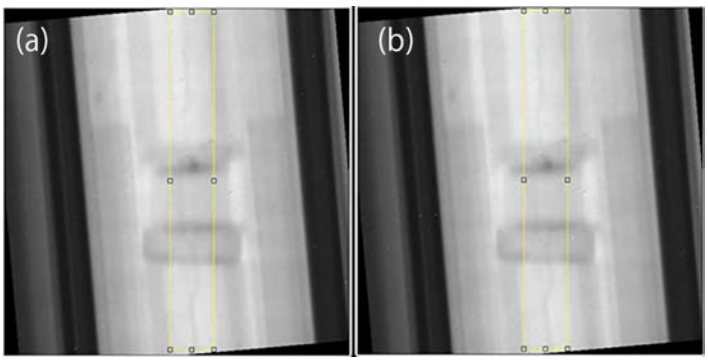

Fig. 1 NR images of test cell consisting of ^{7}Li-LAGP (a) before and (b) after the electrolysis.

RESULTS: Fig. 1 shows the NR images of (a) before and (b) after the electrolysis. The dark area indicates the ^{6}Li-containing part (electrode) in the test cell and the intermediate area between the electrodes corresponds to the electrolyte. Fig. 2 (a) shows the neutron-transmitted intensities of the image before and after the electrolysis. Since the difference is relatively small, the data before the electrolysis are divided by those after the electrolysis in (b). A large deviation is observed around the anode interface, indicating that ^{6}Li is extracted from the anode and migrated into the electrolyte around the anode side.

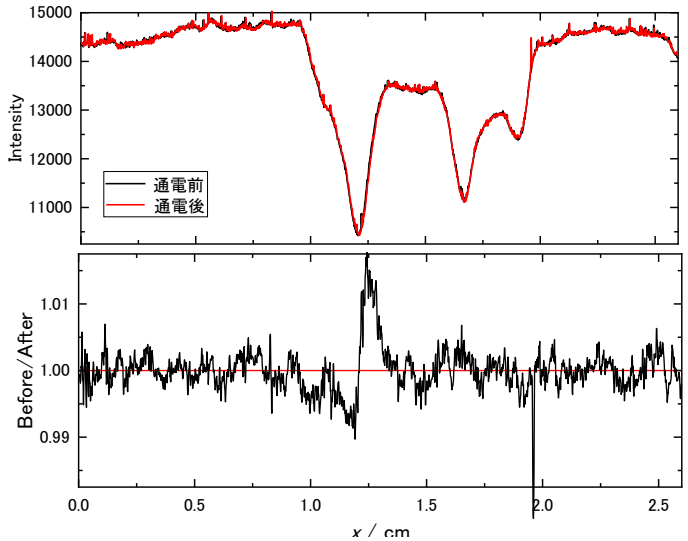

Fig. 2 (a) Neutron intensity profiles for the test cell before and after the electrolysis. (b) Division intensities of the cell.

Flow Visualization of Coolant inside Layerd Rod Array

M. Kaneda[1], Y. Uemura[2] and K. Suga[1]

[1]*Department of Mechanical Engineering, Osaka Metropolitan University*
[2]*Faculty of Mechanical Engineering, Osaka Prefecture University*

INTRODUCTION: Trend of electric motors in electric and hybrid vehicles is higher rotation speed, more power, and compactness [1]. This leads higher heat density due to Joule heating of electric coil in the compact motor package. One of present cooling techniques is so-called direct cooling that the coolant is poured directly onto the coil from a nozzle above. Wetting and profile of the coolant are crucial for the cooling efficiency. We experimented the visualization of the coolant liquid inside the layered structure last year. We found the profile of the coolant inside the structure depends on the pouring liquid temperature and flowrate rather than the applied heat on the structure. In this study, effects of the liquid temperature and flowrate on the liquid profile are further investigated by the neutron radiography.

EXPERIMENTS: The coolant liquid (Automatic Transmission Oil) pumped up from the bath was poured onto the horizontal simplified coil structure. The coolant temperature and flowrate are controlled constant by thermostatic bath and electric pump. The coil structure was presumed by the four-layered accumulated serpentine aluminum plates. The coolant temperature at the nozzle was set at 35 and 50 deg.C and the flowrates of the coolant were tested at 500 and 650 mL/min. The neutron radiography was conducted in B-4 room and visualized inside the structure from the horizontal direction.

RESULTS: The representative visualized images are shown in Fig. 1. The poured liquid spreads as it goes down through the layer. As the liquid temperature increases under the constant coolant flowrate, the liquid profile inside the structure shrinks due to the lower viscosity. As the flowrate becomes larger at the constant liquid temperature, the liquid inside the structure becomes large since the liquid at the uppermost layer spreads. The results obtained have good agreement with our previous trial.

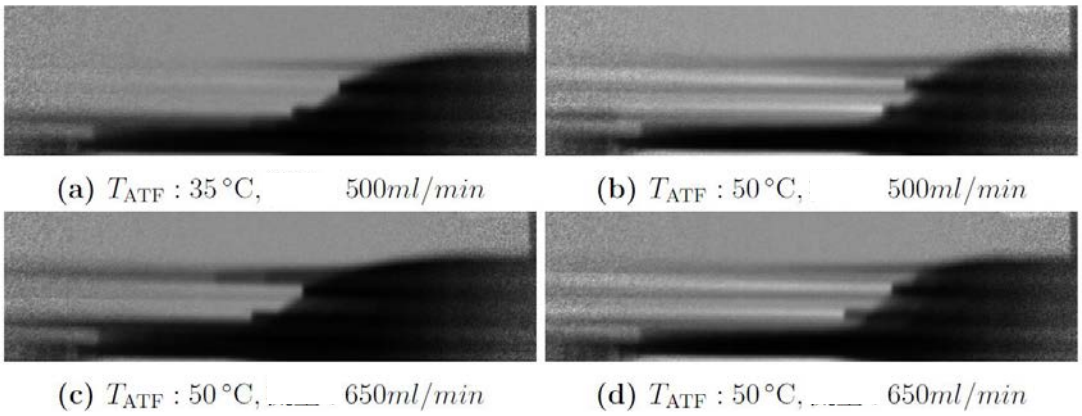

Fig. 1. Visualized images of the coolant inside the layered structure.

REFERENCES:

[1] N. Kobayashi and T. Ikegami, Thermal Sci. Eng., **15(2)** (2007) 49-54.